Inorg. Chem. **2008**, *47*, 6880−6888

Substituted β-Cyclodextrin and Calix[4]arene As Encapsulatory Vehicles for Platinum(II)-Based DNA Intercalators

Anwen M. Krause-Heuer,[†] Nial J. Wheate,[†] Michael J. Tilby,[‡] D. Graham Pearson,[§] Christopher J. Ottley,[§] and Janice R. Aldrich-Wright*[,†]

School of Biomedical and Health Sciences, University of Western Sydney, Locked Bag 1797, Penrith South DC, 1797, NSW, Australia, Northern Institute of Cancer Research, Paul O'Gorman Building, Medical School, Framlington Place, University of Newcastle Upon Tyne, Newcastle Upon Tyne, NE2 4HH, United Kingdom, and Arthur Holmes Isotope Geology Laboratory, Department of Earth Sciences, University of Durham, Science Laboratories, South Road, Durham City, DH1 3LE, United Kingdom

Received March 13, 2008

The encapsulation of three platinum(II)-based anticancer complexes, [(5,6-dimethyl-1,10-phenanthroline)(1*S*,2*S*-diaminocyclohexane)platinum(II)]$^{2+}$ (**56MESS**), [(5,6-dimethyl-1,10-phenanthroline)(1*R*,2*R*-diaminocyclohexane)platinum(II)]$^{2+}$ (**56MERR**), and [(5,6-dimethyl-1,10-phenanthroline)(ethylenediamine)platinum(II)]$^{2+}$ (**56MEEN**), with carboxylated-β-cyclodextrin (c-β-CD) and *p*-sulfonatocalix[4]arene (s-CX[4]) has been examined by one- and two-dimensional ^{1}H nuclear magnetic resonance (NMR) spectroscopy, pulsed gradient spin−echo NMR, ultraviolet spectrophotometry, glutathione degradation experiments, and growth inhibition assays. Titration of any of the three metal complexes with c-β-CD resulted in 1:1 encapsulation complexes with the cyclodextrin located over the intercalating ligand of the metal complexes, with a binding constant of 10^4-10^5 M^{-1}. In addition to binding over the phenanthroline ligand of **56MEEN**, c-β-CD was also found to portal bind to the ethylenediamine ligand, with fast exchange kinetics on the NMR timescale between the two binding sites. In contrast, the three metal complexes all formed 2:2 inclusion complexes with s-CX[4] where the two metal complexes stacked in a head-to-tail configuration and were capped by the s-CX[4] molecules. Interestingly, the **56MEEN**-s-CX[4] complex appeared to undergo a thermodynamically controlled rearrangement to a less soluble complex over time. Encapsulation of the metal complexes in either c-β-CD or s-CX[4] significantly decreased the metal complexes' rate of diffusion, consistent with the formation of larger particle volumes. Encapsulation of **56MESS** within s-CX[4] or c-β-CD protected the metal complex from degradation by reduced *L*-glutathione, with a reaction half-life greater than 9 days. In vitro growth inhibition assays using the LoVo human colorectal cancer cell line showed no significant change in the cytotoxicity of **56MESS** when encapsulated by either s-CX[4] or c-β-CD.

Introduction

A family of platinum(II)-based DNA intercalators based on the 1,10-phenanthroline intercalating ligand and the 1,2-diaminocyclohexane ancillary ligand has been developed by our group as potential anticancer drugs.[1−3] The lead complex, [(5,6-dimethyl-1,10-phenanthroline)(1*S*,2*S*-diaminocyclohexane)platinum(II)]$^{2+}$ (**56MESS**, Figure 1) displays cytotoxicity up to 100-fold greater than cisplatin.[2] The stereochemistry of the ancillary ligand has been shown to influence the cytotoxicity of the metal complexes, with **56MESS** more cytotoxic than [(5,6-dimethyl-1,10-phenanthroline)(1*R*,2*R*-diaminocyclohexane)platinum(II)]$^{2+}$ (**56MERR**) and the achiral [(5,6-dimethyl-1,10-phenanthroline)(ethylenediamine)-platinum(II)]$^{2+}$ (**56MEEN**), respectively.[2,3]

Drug degradation is an issue which affects the anticancer activity of many metal complexes. Platinum based anticancer drugs, such as cisplatin and carboplatin, are known to be readily degraded into nonactive complexes by glutathione (γ-glutamylcysteinylglycine) and proteins containing me-

* To whom correspondence should be addressed. E-mail: j.aldrich-wright@uws.edu.au. Phone: +61 2 4620 3218. Fax: +61 2 4620 3025.
† University of Western Sydney.
‡ University of Newcastle Upon Tyne.
§ University of Durham.

10.1021/ic800467c CCC: $40.75
Published on Web 07/02/2008

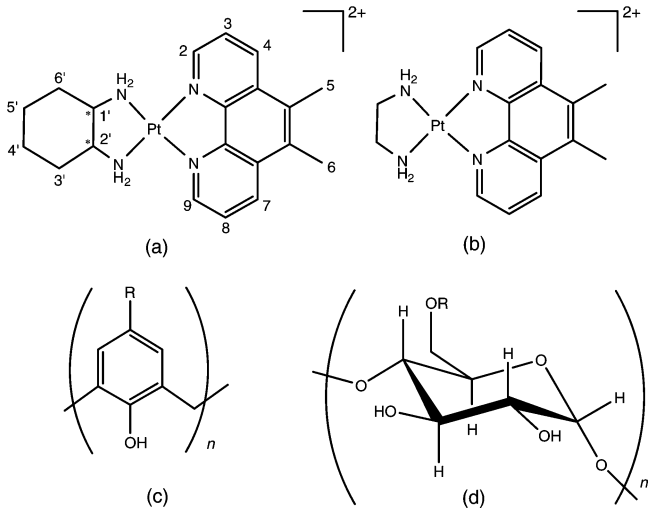

Figure 1. Chemical structures of the platinum(II)-based DNA intercalators: (a) **56MESS/56MERR**, showing the numbering system adopted; (b) **56MEEN**; (c) calix[*n*]arene (where $n = 4$, 6 or 8), in nonsubstituted calix[*n*]arene, R = H, while in s-CX[4], R = SO_3Na; and (d) *n*-cyclodextrin (where $n = 6$, 7 or 8), in β-CD R = H, in c-β-CD R = H or CH_2COOH. * Indicates a chiral center of the metal complex, either *R* or *S*. Anions have been omitted for clarity but are generally chlorides.

thionine or cysteine residues.[4] Recently, we have reported a detailed examination of the degradation of our metal complexes by reduced *L*-glutathione and, to a lesser extent, *L*-methionine.[5] From this study we hypothesized that if degradation could be slowed or even prevented, then it may be possible to increase the activity of the metal complexes. As such we have been examining possible methods of encapsulating our platinum(II)-based DNA intercalators to protect them from in vitro/in vivo degradation, using glutathione as a model for potential degradative mechanisms that could occur.

One such family of encapsulation vehicles are cucurbit[*n*]urils (CB[*n*]) which are barrel shaped molecules that consist of repeating glycoluril subunits connected by two methylene bridges.[6] Partial encapsulation of **56MESS**, **56MERR**, and **56MEEN** by CB[*n*]s has been shown to stop their degradation by glutathione.[5] This makes CB[*n*]s potentially useful as protective delivery vehicles; however, the resultant encapsulation complexes have limited water solubility and in some cases CB[*n*] encapsulation can significantly affect the cytotoxicity of the metal complexes.[7] For these reasons, a number of other molecular hosts are being investigated as potential alternatives, including calix[*n*]arenes and cyclodextrins.

Calix[*n*]arenes (CX[*n*]) are cyclic oligomers of repeating phenolic units joined via methylene bridges where the number of monomers is 4, 6 or 8 (Figure 1).[8] Unsubstituted CX[*n*]s are not water soluble, and as such, research utilizing this group of molecules as drug delivery vehicles has focused on substituted CX[*n*], particularly the *p*-sulfonatocalix[*n*]arenes, as they possess the highest solubility of commercially available CX[*n*] derivatives.[9] The interior surface and sulfonate groups provide association sites for both hydrophobic and hydrophilic molecules, respectively.

Cyclodextrins (*n*-CD) are a water soluble family of cyclic oligosaccharides that are composed of α-*D*-glucose units joined by α-1,4-linkages (Figure 1).[10] The three most common *n*-CDs consist of 6, 7, or 8 monomers and are named α-, β-, and γ-cyclodextrin, respectively. *n*-CDs have a toroidal basket shape with a hydrophobic internal cavity, allowing them to form noncovalent encapsulation complexes with a variety of compounds.[10,11] A large family of chemically modified cyclodextrins has been developed, and factors such as the degree of substitution, the size of the functional groups, and the charge on the molecules have been shown to influence significantly the formation of host−guest complexes in drug delivery.[12]

In this study we examined the encapsulation of **56MESS**, **56MERR**, and **56MEEN** with *p*-sulfonatocalix[4]arene (s-CX[4]) and carboxylated-β-CD (c-β-CD) using one- and two-dimensional ^{1}H nuclear magnetic resonance (NMR) spectroscopy, pulsed gradient spin−echo (PGSE) NMR, and ultraviolet (UV) spectrophotometry. We also studied the effects of encapsulation on degradation by reduced *L*-glutathione, and on the cytotoxicity of **56MESS** using in vitro growth inhibition assays.

Experimental Section

Materials. The platinum(II) complexes, **56MESS**, **56MERR**, and **56MEEN**, were synthesized as previously described.[2] Deuterated solvents D_2O (99.9%) and d_6-DMSO (99.9%) were purchased from Cambridge Isotope Laboratories. CX[6], s-CX[4], reduced *L*-glutathione, α-, β-, γ-, and c-β-CD were purchased from Sigma-Aldrich. Foetal calf serum, *L*-glutamine, RPMI Medium 1640 (HEPES Modification, without *L*-glutamine) and trypsin EDTA concentrate were purchased from Sigma. The human colorectal cancer (LoVo) cell line was purchased from the American type Culture Collection. All general solvents were used as provided and were of analytical grade or better.

(1) (a) Wheate, N. J.; Brodie, C. R.; Collins, J. G.; Kemp, S.; Aldrich-Wright, J. R. *Mini Rev. Med. Chem.* **2007**, *7*, 627–648. (b) Jaramillo, D.; Buck, D. P.; Collins, J. G.; Fenton, R. R.; Stootman, F. H.; Wheate, N. J.; Aldrich-Wright, J. R. *Eur. J. Inorg. Chem.* **2006**, 839–849. (c) Brodie, C. R.; Turner, P.; Wheate, N. J.; Aldrich-Wright, J. R. *Acta Crystallogr.* **2006**, *E62*, m3137–m3139. (d) Brodie, C. R.; Collins, J. G.; Aldrich-Wright, J. R. *Dalton Trans.* **2004**, 1145–1152. (e) Fisher, D. M.; Bednarski, P. J.; Grunert, R.; Turner, P.; Fenton, R. R.; Aldrich-Wright, J. R. *ChemMedChem* **2007**, *2*, 488–495. (f) Collins, J. G.; Rixon, R. M.; Aldrich-Wright, J. R. *Inorg. Chem.* **2000**, *39*, 4377–4379.
(2) Wheate, N. J.; Taleb, R. I.; Krause-Heuer, A. M.; Cook, R. L.; Wang, S.; Higgins, V. J.; Aldrich-Wright, J. R. *Dalton Trans.* **2007**, 5055–5064.
(3) Kemp, S.; Wheate, N. J.; Buck, D. P.; Nikac, M.; Collins, J. G.; Aldrich-Wright, J. R. *J. Inorg. Biochem.* **2007**, *101*, 1049–1058.
(4) Reedijk, J. *Chem. Rev.* **1999**, *99*, 2499–2510.
(5) Kemp, S.; Wheate, N. J.; Pisani, M. P.; Aldrich-Wright, J. R. *J. Med. Chem.* **2008**, *51*, 2787–2794.
(6) Lagona, J.; Mukhopadhyay, P.; Chakrabarti, S.; Isaacs, L. *Angew. Chem., Int. Ed.* **2005**, *44*, 4844–4870.
(7) Kemp, S.; Wheate, N. J.; Wang, S.; Collins, J. G.; Ralph, S. F.; Day, A. I.; Higgins, V. J.; Aldrich-Wright, J. R. *J. Biol. Inorg. Chem.* **2007**, *12*, 969–979.
(8) Gutshe, C. D. *The Characterisation and Properties of Calixarenes*; The Royal Society of Chemistry: Cambridge, 1989.
(9) Arduini, A.; Pochini, A.; Reverberi, S.; Ungaro, R. *J. Chem. Soc., Chem. Commun.* **1984**, 981–982.
(10) Bender, M. L.; Kominyama, M. *Cyclodextrin Chemistry*; Springer-Verlag: Berlin, 1978.
(11) Stejtli, J. *Cyclodextrins and Their Inclusion Complexes*; Akademiai Kiado: Budapest, 1982.
(12) Wenz, G. *Angew. Chem., Int. Ed. Engl.* **1994**, *33*, 803–822.

Nuclear Magnetic Resonance. One- and two-dimensional NMR spectra were obtained on either a 300 MHz Varian Mercury spectrometer or a 400 MHz Bruker Avance spectrometer in D_2O, referenced internally to the solvent. ^{1}H NMR experiments were conducted at 25 °C unless otherwise specified. For one-dimensional spectra, a spectral width of 7000 Hz was used with 50 000 data points and a relaxation delay of 3.7 s. Two-dimensional nuclear Overhauser effect spectra (NOESY) were obtained using a spectral width of 7 000 Hz with 256 increments in the t1 dimension, 2048 points in the t2 dimension, a mixing time of 0.5−0.8 s and a relaxation delay of 5 s. The diaminocyclohexane resonances of **56MESS** and **56MERR** in the absence and presence of s-CX[4] were assigned by correlated spectroscopy (COSY) NMR.

NMR Titration Experiments. NMR samples were prepared from a stock solution of metal complex (∼20 mM, D_2O) by diluting with D_2O to a concentration between 0.5 to 2.0 mM and a total volume of 600 μL. Solutions of s-CX[4] or c-β-CD were added incrementally (5 μL, ∼ 40 mM) to the metal complexes until the desired host−guest ratio was reached. ^{1}H NMR spectra were recorded at each titration point.

Host−guest Complex Solubility. The solubility of the host−guest complexes was determined by the preparation of equimolar concentrations of metal complex and guest in water. The two solids were combined in a sample vial, and water was titrated in 10 to 100 μL increments until no visible solid remained.

Determination of Diffusion Coefficients. ^{1}H PGSE NMR experiments were performed using a Hahn spin-echo PGSE pulse sequence optimized to reduce signal loss due to spin−spin relaxation,[13] using a sweep width of 5000 Hz, 32−256 scans, a Δ of 25−250 ms, a δ of 1.5−10 ms, and with 16 gradient increments (0−0.41 Tm^{-1}). The diffusion coefficient was determined from a nonlinear least-squares regression of $E = \exp(\gamma^2 g^2 \delta^2 D(\Delta - \delta/3))$ onto a plot of the resonance integration at each gradient increment compared to the integration at zero gradient as a function of $\gamma^2 g^2 \delta^2 D(\Delta - \delta/3)$.

UV−vis. Absorbance spectra were recorded on a Cary 1E spectrophotometer at room temperature in the range 200−400 nm, using a 1 cm quartz cell. All samples were automatically corrected for solvent baseline. Titrations were performed by the incremental addition of host (1 μL, 2.9 mM) into solutions of metal complex (3.000 mL, 25 μM) with thorough mixing by inversion before recording the spectrum at each titration point. The change in the UV spectrum of the metal complexes with s-CX[4] was calculated by the subtraction of the UV spectrum of free s-CX[4] from that of the metal complex with s-CX[4] at each titration point.

Absorbances for samples from the growth inhibition assays were obtained on a Dynex Technologies Spectra MR plate reader using Revelation software, measured at 490 and 570 nm [570 nm is the peak of highest intensity of the SRB compound, however, with high cell proliferation the absorption at this wavelength is often above the limit of detection of the instrument. As such the absorbance is also measured at the shoulder peak at 490 nm. The wavelength for calculation of IC_{50} is chosen based on an optimal maximal absorbance of 0.7−1.0 A.U.]. Absorbances were corrected by the subtraction of the absorbance of the blanks (containing no LoVo cells).

(13) Price, W. S. *Concepts Magn. Reson.* **1997**, *9*, 299–336.

Binding Constants. Binding constants were calculated using Scatchard plots,[14,15] the double-reciprocal method,[14,15] nonlinear least-squares regression,[14] and the intrinsic method.[16]

For the titration of host into a solution of guest, the relationship between the change in absorbance of the guest and the host concentration is given by[14,15]

$$\frac{A - A_0}{[H]} = (A_\infty - A_0)K - (A - A_0)K \qquad (1)$$

where A_0 is the absorbance of the guest in the absence of host, $[H]$ is the concentration of host at each titration point, A_∞ is the absorbance when all the guest molecules are complexed by host (i.e., guest with large excess of host), A is the observed absorbance at each titration point, and K is the binding constant (M^{-1}).

From eq 1, a plot of $(A - A_0)/[H]$ versus $A - A_0$ (i.e., a Scatchard plot) was the first method used for the estimation of the binding constant. A linear plot suggests a 1:1 binding stoichiometry, where the binding strength is directly related to the concentration of host, and the negative value of the gradient is the binding constant. A nonlinear plot indicates the formation of higher order host−guest complexes.[14]

Equation 1 can also be rearranged into the Benesi−Hildebrand form:[14,15]

$$\frac{1}{A - A_0} = \frac{1}{(A_\infty - A_0)K[H]} + \frac{1}{A_\infty - A_0} \qquad (2)$$

From eq 2, linear regression on a plot of $1/(A - A_0)$ versus $1/[H]$ (i.e., a double-reciprocal plot) provides an estimate of the binding constant, with $K = y$-intercept/gradient. Again, a linear plot suggests a 1:1 binding mode, while a nonlinear plot indicates a higher order complex.[17] The double-reciprocal method, however, places more emphasis on lower concentration values compared with the Scatchard plot, as the slope of the line is now more sensitive to the data point at the lowest concentration.[14]

Further rearrangement of eq 1 and 2 gives the direct relationship between the observed absorbance and host concentration:

$$A = A_0 + \frac{(A_\infty - A_0)K[H]}{1 + K[H]} \qquad (3)$$

The binding constant can be determined using nonlinear least-squares regression of eq 3 onto the experimental data (Origin Pro 7.5). Initial parameter estimates of K and A_∞ required for the analysis were obtained from the Scatchard and double-reciprocal plots.

The intrinsic method, developed by Rodger and Nordén[16] is given by:

$$\frac{H^k_{tot} - H^j_{tot}}{\rho^k - \rho^j} = \frac{G_{tot}}{\alpha}\left(\frac{\dfrac{H^k_{tot}}{\rho^k} - \dfrac{H^j_{tot}}{\rho^j}}{\rho^k - \rho^j}\right) + \alpha \qquad (4)$$

where H_{tot} is the concentration of host at any given titration point, ρ is the absorbance at a titration point, G_{tot} is the concentration of guest (which remains constant), j and k are any two titration points, and α is a constant over the range of binding ratios.

(14) Muñoz de la Peña, A.; Salinas, F.; Gomez, M. J.; Acedo, M. I.; Sánchez Peña, M. *J. Inclusion Phenom. Mol. Recognit. Chem.* **1993**, *15*, 131–143.
(15) Connors, K. A. *Binding Constants: The Measurements of Molecular Complex Stability*; Wiley: New York, 1987.
(16) Rodger, A.; Nordén, B. *Circular Dichroism and Linear Dichroism*; Oxford University Press: Great Britain, 1997.
(17) Wagner, B. D.; Boland, P. G.; Lagona, J.; Isaacs, L. *J. Phys. Chem. B* **2005**, *109*, 7686–7691.

Using repeated application of eq 4 for each incremental titration point, the intrinsic plot of $(H^k_{tot} - H^i_{tot})/(\rho^k - \rho^i)$ versus $[(H^k_{tot}/\rho^k) - (H^i_{tot}/\rho^i)]/(\rho^k - \rho^i))$ should be a straight line with a slope of G_{tot}/α and y-intercept of α. α (given by $\alpha = G_b/\rho$) is used to calculate the concentration of bound (G_b) and free (G_f) guest for each aliquot of host added (where $G_{tot} = G_f + G_b$), and these values are then applied in a Scatchard plot of G_b/H versus $(G_b/H)/G_f$, where the negative value of the gradient is K. This method uses the value of α at every titration point to calculate an average value and also does not rely on an estimation of A_∞, which makes this a more accurate method than the other three preceding methods.

Glutathione Degradation. The metal complexes (1 mM) were combined with s-CX[4] or c-β-CD (1 mM) and reacted with reduced *L*-glutathione (4 mM) in unbuffered D_2O at 37 °C before ^{1}H NMR spectra were obtained at regular intervals over a period of 9 days.[5] [The concentration of *L*-glutathione used for our model degradation experiments (4 mM) was mid range for the *L*-glutathione concentration (0.5−10 mM) that is present in cells.[19]] The half-lives ($t_{1/2}$) of the degradation reactions were determined from a plot of the percent of undegraded metal complex as a function of time (h).

Growth Inhibition Assays. In a modification of a previously published method,[18] cells were grown in RPMI Medium 1640, HEPES Modification containing fetal calf serum (10% v/v) and *L*-glutamine (300 mg L^{-1}) at 37 °C and in a 5% CO_2 atmosphere. Cells were released from culture flasks using trypsin and resuspended in full medium. After counting using a hemocytometer the cells were inoculated into 96-well plates (1000 cells in 100 μL of medium per well). Following inoculation, the plates were incubated for 24 h before being used to evaluate the effect of the metal complexes on cell growth.

Stock solutions (1 mL, 10 mM) of **56MESS**, s-CX[4] and c-β-CD were prepared in ultra pure water. The solutions were filtered through a 0.22 μm syringe filter into sterile tubes. **56MESS** (10 mM, 200 μL) was combined with s-CX[4], c-β-CD (10 mM, 200 μL) or filter sterilized water (200 μL), resulting in 5 mM solutions of **56MESS**, **56MESS**–s-CX[4], and **56MESS**–c-β-CD. The stock solutions were stored at −20 °C until required for use.

The stock solutions (5 mM) of metal complexes in water were initially diluted 100-fold into culture medium. Sterile NaCl solution was then added to the medium to correct for the resulting change in osmolality. This medium was then diluted with additional medium (supplemented to an equal extent with water and NaCl) to give concentration ranges of the metal complexes such that when aliquots of 100 μL were added to wells of the 96-well plates, the final concentrations were 0.0−1.0 μM (continuous exposure experiments) or 0.0−40.0 μM (1 h exposure experiments). The plates were incubated with the metal complex solutions for either 1 h or 5 days. Following the 1 h exposure, the medium was removed by aspiration, replaced with 200 μL of fresh medium, and the plates were then incubated for 5 days. All plates were fixed, stained, and read similarly to the previously published method.[18] In brief, the medium was removed and replaced with phosphate buffered saline (PBS, 200 μL per well) before addition of trichloroacetic acid (50 μL per well of 50% w/v solution at 4 °C). After 1 h at 4 °C, the plates were washed with water and sulforhodamine B (SRB) solution [0.4% (w/v) in 1% (v/v) acetic acid] was added (100 μL per well). After 30 min at room temperature the SRB solution was removed and the wells were washed with acetic acid (1% v/v) and then dried. To each well, 100 μL of tris(hydroxymethyl)aminomethane solution (10 mM, pH = 9.5) was added and the absorbance read at 570 and 490 nm. IC_{50} was calculated as the metal complex concentration at which there was 50% inhibition of cell growth relative to the control wells.

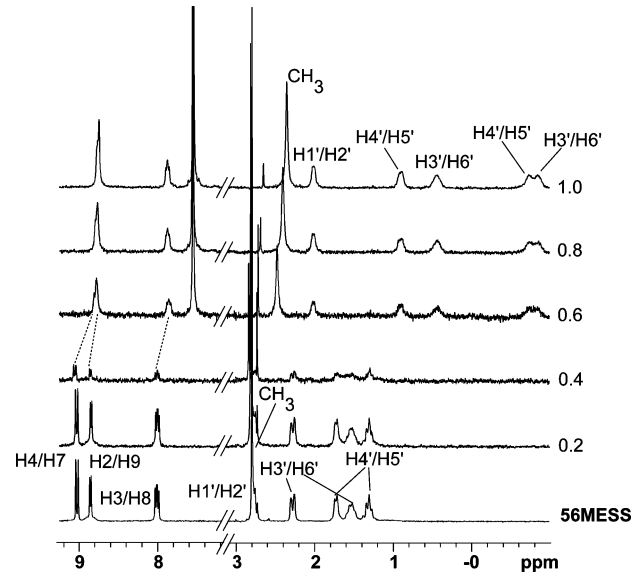

Figure 2. ^{1}H NMR spectra of free **56MESS** and **56MESS** with 0.2−1.0 equiv of s-CX[4], demonstrating the significant upfield shift experienced by the diaminocyclohexane proton resonances. These spectra are indicative of those obtained for **56MERR** and **56MEEN**.

Results and Discussion

The platinum(II)-based DNA intercalator complexes **56MESS**, **56MERR**, and **56MEEN** (2 mM) were initially added to solutions of unsubstituted calix[6]arene and α-, β-, and γ-cyclodextrin in dimethyl sulfoxide and water, respectively. No interaction was observed between any of the unsubstituted macrocycles and the metal complexes. As a consequence, the derivatives s-CX[4] and c-β-CD were investigated as potential hosts. These hosts were chosen because ion−dipole and ion−ion interactions between the metal complexes and the additional functional groups on the substituted macrocycles would make encapsulation more favorable, in addition to the hydrophobic effects of the cavity binding.

s-CX[4]. When s-CX[4] was titrated into solutions of **56MESS**, **56MERR**, and **56MEEN** (D_2O, 2 mM) to equimolar concentrations, significant and specific shifts of the metal complex resonances were observed in the ^{1}H NMR spectra. The initial addition of 0.2 to 0.4 equiv of s-CX[4] to the metal complexes resulted in the formation of a cloudy white precipitate and a decrease in the intensity of the metal complex resonances; however, no significant chemical shift changes were observed (Figure 2). When the s-CX[4] to metal complex ratio was increased to 0.5, the metal complex resonances were drastically reduced in intensity and difficult to observe. After the addition of 0.6 equiv of s-CX[4], the **56MESS** and **56MERR** resonances reappeared and shifted upfield (lower ppm); the diaminocyclohexane resonances shift about 0.7−3.0 ppm while the phenanthroline resonances shifted about 0.1−0.4 ppm (see Figure 3). The largest shift of the diaminocyclohexane resonances was experienced by the H3′/H6′ protons, and the largest shift of the phenanthro-

(18) Meczes, E. L.; Pearson, A. D. J.; Tilby, M. J. *Brit. J. Cancer* **2002**, *86*, 485–489.
(19) Jung, Y.; Lippard, S. *J. Chem. Rev.* **2007**, *107*, 1387–1407.

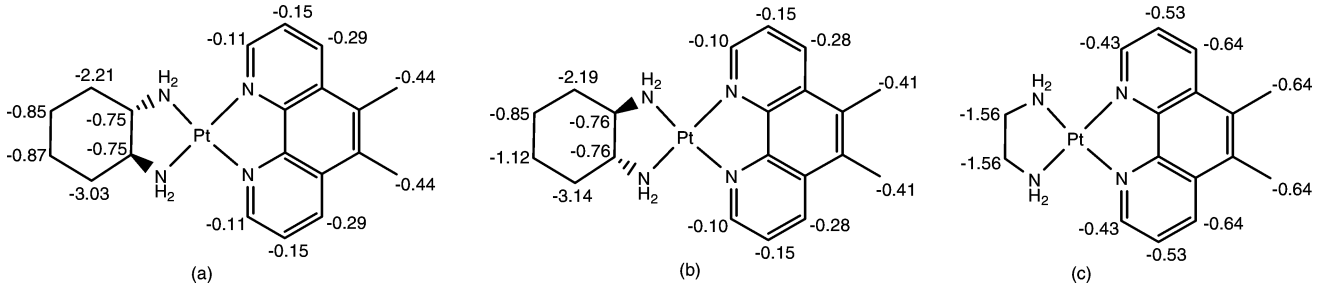

Figure 3. Change in chemical shift experienced by the proton resonances of (a) **56MESS**, (b) **56MERR**, and (c) **56MEEN** after the formation of the 2:2 host−guest complex with s-CX[4]. Large upfield shifts (negative values) are experienced by both the diaminocyclohexane and phenanthroline resonances of the metal complexes upon encapsulation. Charges and counter-ions have been omitted for clarity.

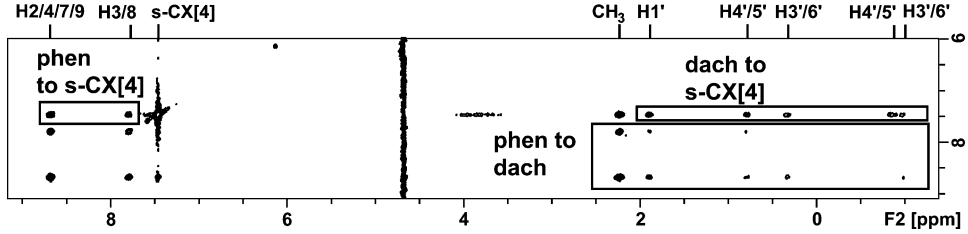

Figure 4. Two-dimensional NOESY spectrum (400 ms) of the 2:2 host−guest complex of s-CX[4] with **56MESS** showing the NOE cross-peaks from the metal complex phenanthroline and diaminocyclohexane resonances to the s-CX[4] aromatic resonance, and the metal complexes' phenanthroline resonances to its own diaminocyclohexane resonances.

line resonances was experienced by the methyl protons. The resonances of **56MEEN** experience similar shifts upfield, with the ethylenediamine resonance shifting 1.5 ppm and the phenanthroline resonances shifting about 0.4−0.7 ppm. The methyl proton signal of **56MEEN** experienced the largest shift (0.64 ppm) of the phenanthroline resonances, as was the case with **56MESS** and **56MERR**. For all three metal complexes the H2/H9 and H4/H7 resonances were superimposed. We interpreted these NMR spectra to mean that the encapsulation follows a two-step process.

The two-dimensional NOESY spectrum of an equimolar solution of s-CX[4] and **56MESS** showed both intra- and intermolecular NOE cross-peaks between the metal complex and the macrocycle (Figure 4). Strong NOEs were seen between the aromatic s-CX[4] proton and all five diaminocyclohexane protons. The superimposed H2/H9 and H4/H7 resonances gave intramolecular cross-peaks to both the H3/H8 and the phenanthroline methyl protons. The H2/H9 and H4/H7 protons also give a strong intermolecular NOEs to the s-CX[4] aromatic proton. Importantly, the **56MESS** H2/H9 and H4/H7 protons also gave NOE cross-peaks to all five **56MESS** diaminocyclohexane protons. No NOEs were observed between the s-CX[4] methylene resonance and the metal complex.

It has previously been reported that upfield shifts in ^{1}H NMR spectra of 1−4 ppm are observed for ionic guests included within the cavity of *p*-sulfonatocalix[4]arenes.[19] The large upfield shifts of the ancillary ligand (diaminocyclohexane, ethylenediamine) resonances in the ^{1}H NMR spectrum when **56MESS**, **56MERR**, and **56MEEN** were combined with s-CX[4] indicate that the s-CX[4] is encapsulated over the ancillary ligand, with the H3′/H6′ situated deepest within the portal (as these proton resonances experience the largest upfield shift). The significant upfield shifts of the phenanthroline resonances also suggests that they are shielded

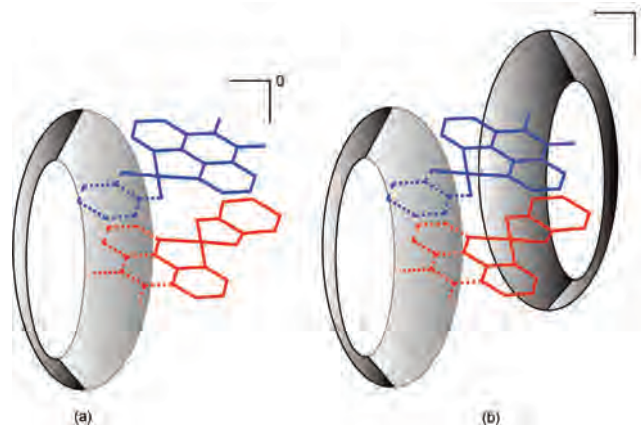

Figure 5. Diagrammatic representation of (a) the 2:1 host−guest complex of **56MESS**–s-CX[4] which carries no net charge which is initially formed at low s-CX[4] to metal complex ratios, and (b) the final anionic 2:2 host−guest complex of **56MESS**–s-CX[4] where two metal complex molecules associate in a head-to-tail fashion, with one s-CX[4] molecule encapsulated over either end. Counter-ions have been omitted for clarity.

within a s-CX[4], with the methyl protons situated deepest within the cavity. This is supported by the NOESY spectrum, with cross-peaks observed from the aromatic s-CX[4] resonance to both the aromatic and diaminocyclohexane resonances of the metal complexes. Cross-peaks between the diaminocyclohexane and phenanthroline resonances suggest the formation of a head-to-tail type dimer between two metal complex molecules, encapsulated at either end by an s-CX[4] molecule; that is, a 2:2 host−guest complex (Figure 5). This provides an explanation as to why the metal complex resonances are drastically reduced in intensity in the ^{1}H NMR spectrum of s-CX[4] and metal complex when the ratio of host to guest is less than 1. At this ratio, in solution, there are two drug molecules for every s-CX[4] molecule, thus ion-pairing gives a neutral complex which is subsequently poorly soluble (see Figure 5). As s-CX[4] is added from 0.6

Table 1. Diffusion Coefficients of **56MESS**, **56MERR**, and **56MEEN** in the Absence and Presence of an Equimolar Concentration of s-CX[4] (0.5 mM) or c-β-CD (2 mM) in D_2O

	diffusion coefficient ($\times 10^{-10}$ m^2 s^{-1})			
	s-CX[4]		**c-β-CD**	
metal complex	free	bound	free	bound
56MESS	4.17 ± 0.01	2.62 ± 0.06	4.00 ± 0.01	2.07 ± 0.02
56MERR	4.17 ± 0.01	2.64 ± 0.02	4.10 ± 0.04	2.01 ± 0.06
56MEEN	*n.d.*	*n.d.*	4.81 ± 0.06	2.28 ± 0.05

[n.d.] Could not be determined.

to 1.0 equiv of metal complex, the complex is resolubilized as a second s-CX[4] molecule binds over the metal complex dimer, resulting in a net 4- charge (Figure 5).

The diffusion coefficient of the metal complexes was measured using pulsed gradient spin–echo (PGSE) NMR. The experiments were conducted at a concentration of 0.5 mM because higher concentrations resulted in the formation of large amounts of precipitate. The solutions appeared slightly cloudy; however, lower concentrations resulted in large experimental running times. The diffusion coefficients of **56MESS** and **56MERR** are significantly smaller when combined with s-CX[4] (Table 1). The diffusion coefficient of s-CX[4] when bound to the metal complexes is also significantly smaller compared to free s-CX[4] (3.21×10^{-9} m^2 s^{-1}). These reduced diffusion coefficients further confirm that host−guest complexes have been formed, as the larger metal complex–s-CX[4] complexes are expected to diffuse slower (because of their larger volumes) compared with the free metal complexes. The diffusion coefficient of **56MEEN** with s-CX[4] could not be measured accurately at 0.5 mM or lower concentrations, as the ^{1}H resonances had reduced significantly in intensity during the experimental running time. This may be due to the initial 2:2 host−guest complex undergoing a rearrangement over time, and forming a less soluble complex (for which a structure could not be determined).

The formation of the 2:2 host−guest complexes of s-CX[4] were further examined by UV spectrophotometry. When 0.04 to 1.20 equiv of s-CX[4] were titrated into solutions of **56MESS**, **56MERR**, or **56MEEN** (∼25 μM), significant changes were noted in the UV spectra in the range 200−320 nm. As both the metal complex and the s-CX[4] absorb strongly in this region, the changes in the UV spectra of the metal complexes were determined by the subtraction of the absorbance of free s-CX[4] from that of the metal complex with s-CX[4] at each titration point. For **56MESS** and **56MERR**, up to and including 0.40 equiv of s-CX[4], the absorbance maximum at 286 nm decreased in intensity with increasing s-CX[4] concentration, along with a 1 nm bathochromic shift. From 0.44 to 1.20 equiv of s-CX[4] the absorbance maximum of **56MESS** and **56MERR** at 285 nm increased in intensity (Figure 6).

A plot of the metal complex absorbance at 286 nm versus mole equiv of s-CX[4] demonstrates that encapsulation follows a two-step process (Figure 6a). The two linear regions of the double-reciprocal plot of $1/(A - A_0)$ versus 1/[s-CX[4]] also clearly indicates two different binding events, with the overall nonlinear relationship demonstrating that the binding stoichiometry for **56MESS** and s-CX[4] is not 1:1 (Figure 6a inset). This is also supported by the nonlinear nature of the Scatchard plot, indicating the formation of a higher order host−guest complex (in supplementary data). The UV titration of **56MERR** with s-CX[4] proved very similar to that of **56MESS**. This was expected, as calix[*n*]arenes are not chiral compounds, and therefore are not expected to interact stereospecifically with one metal complex compared with the other.

The results for **56MEEN** with s-CX[4] are slightly different. The binding curve from the UV titration at 286 nm of **56MEEN** with s-CX[4] shows a large decrease in absorbance from 0.0 to 0.52 equiv of s-CX[4], followed by a slight increase from 0.56 to 1.20 equiv (see Figure 6b). Like those for **56MESS** and **56MERR**, the overall double-reciprocal plot was not linear (Figure 6b inset). While the Scatchard plot is also nonlinear, it has a distinctly different shape to the plots of **56MESS** and **56MERR** with s-CX[4] (in supplementary data). For **56MESS** and **56MERR**, the absorbance over 200−220 nm decreased and then increased again past 0.4 equiv of s-CX[4]. The maximum change in absorbance in this region was approximately 0.4 A.U. In the **56MEEN** spectra, the decrease in absorbance is larger (0.9 A.U., data not shown) in the region 200−220 nm. The maximum change in absorbance at 286 nm is also substantially higher for **56MEEN** (∼0.5 A.U.) than for **56MESS** and **56MERR** (∼0.2 A.U.), which suggests stronger binding and/or a different equilibrium for the **56MEEN**–s-CX[4] host−guest complex.

The complexes formed by **56MESS** and **56MEEN** with s-CX[4] were monitored by UV spectroscopy over a period of 48 h, over which time the intensity of the **56MEEN** spectrum is significantly reduced, while the **56MESS** spectrum displays no change. The rate of rearrangement of the **56MEEN**–s-CX[4] complex is also increased with heating. Because of the two-step formation of the 2:2 complex, binding constants could not be accurately calculated.

c-β-CD. When c-β-CD was titrated into solutions of **56MESS**, **56MERR**, and **56MEEN** (D_2O, 2 mM), to equimolar concentrations there were significant and specific shifts of the metal complexes' phenanthroline resonances in the ^{1}H NMR spectra (Figure 7). The methyl and H4/H7 proton resonances experienced an upfield shift of about 0.3−0.5 ppm and about 0.2 ppm, respectively. The H2/H9 and H3/H8 resonances both experienced a slight downfield shift of about 0.1 ppm. No significant shift of the diaminocyclohexane resonances of **56MESS/56MERR** was observed; however, a downfield shift of the **56MEEN** ethylenediamine resonance was observed. Chemical shift changes of the c-β-CD resonances were unable to be detected as c-β-CD is a randomly substituted compound, and as such, displays relatively broad resonances. The significant shifts of the phenanthroline resonances in the ^{1}H NMR spectra are suggestive of c-β-CD binding over the phenanthroline ligand of the metal complexes (Figure 7). The additional downfield shift of the ethylenediamine resonance of **56MEEN** suggests that cavity binding is occurring between the c-β-CD and the ancillary ligand of the metal complex (Figures 7 and 8). As

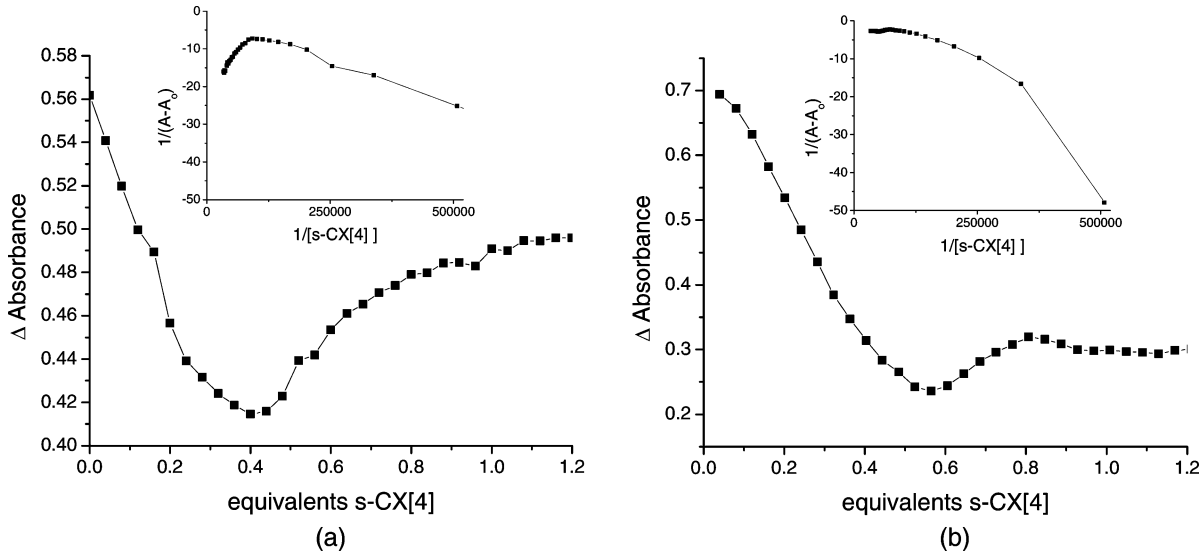

Figure 6. Plot of the change in absorbance (at 286 nm) of (a) **56MESS** and (b) **56MEEN** upon the addition of s-CX[4]. For both metal complexes, two distinct binding events are observed, one from ~0−0.5 equiv, the other from ~0.5−1.20 equiv of s-CX[4] demonstrating the formation of a 2:2 host−guest complex. The insets show the double-reciprocal plots.

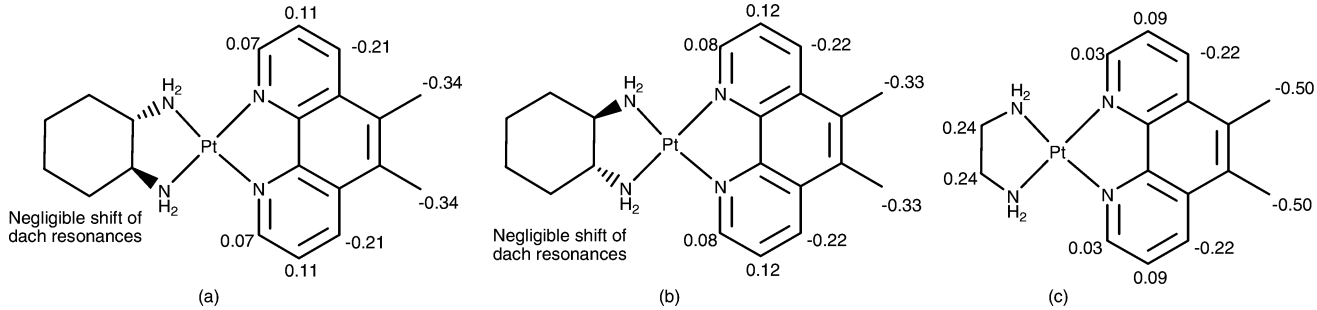

Figure 7. Change in chemical shift experienced by the proton resonances of (a) **56MESS**, (b) **56MERR**, and (c) **56MEEN** when combined with c-β-CD to form 1:1 host−guest complexes. Upfield shifts (negative values) are observed by the phenanthroline methyl and H4/H7 resonances when located within the c-β-CD cavity.

only one set of metal complex resonances is observed at each titration point, the resultant host−guest complexes are in fast exchange on the ^{1}H NMR time scale. Unlike s-CX[4] which forms a 2:2 host−guest complex with the metal complex, c-β-CD only forms 1:1 host−guest complexes. A 2D NOESY experiment of the host−guest complex of c-β-CD and **56MESS** (2 mM) was inconclusive because it only showed intramolecular NOEs for both the c-β-CD and the **56MESS**, but no intermolecular connectivities were observed.

Partial encapsulation of the three metal complexes was also confirmed using NMR diffusion measurements. The formation of the 1:1 host−guest complex of c-β-CD with each of the metal complexes results in a significant decrease in their rate of diffusion, as measured by their diffusion coefficients (Table 1).

When c-β-CD was titrated into solutions of all three metal complexes (25 μM) to a metal complex to c-β-CD ratio of 1:1.2, significant changes were observed in the UV spectra of the metal complexes in the range 200−400 nm. A decrease in the metal complexes' absorbance and a 1 nm bathochromic shift of each maxima at 229 and 285 nm was observed. Saturation was reached at approximately 0.9 equiv (i.e., Figure 9). A double reciprocal plot of $1/(A - A_0)$ against 1/[c-β-CD] yields a linear relationship, which confirms the proposed 1:1 binding mode. Binding constants were calculated using four different methods and for all three metal complexes were found to be 10^4-10^5 M^{-1} (Table 2).

Glutathione Degradation. We have recently shown that **56MESS**, **56MERR**, and **56MEEN** are degraded by reduced *L*-glutathione and *L*-methionine into noncytotoxic complexes, and the rate of degradation was found to be inversely proportional to the metal complexes' cytotoxicity.[5] This indicated that reactivity/stability is likely to play a role in the anticancer structure−activity relationship of this family of metal complexes. Therefore, if degradation of the metal complexes by thiols can be slowed or even stopped, the cytotoxicity and/or efficacy may be improved.

The degradation half-life of **56MESS** with reduced *L*-glutathione has previously been determined to be 68 h compared with cisplatin at 3.3 h.[5] When **56MESS** was combined with 1 equiv of either s-CX[4] or c-β-CD and 4 equiv reduced *L*-glutathione under the same conditions, the half-lifes increase to more than 9 days. The mechanism of degradation of **56MESS**, **56MERR**, and **56MEEN** by *L*-glutathione is via displacement of the metal complex ancillary ligands to form a dinuclear, doubly bridged complex.[5] As s-CX[4] is bound over both the phenanthroline and the ancillary ligands of the metal complexes it is not surprising that is it able to stop degradation. We have shown, however, that c-β-CD encapsulates the metal complexes predominantly over their phenanthroline ligands, so

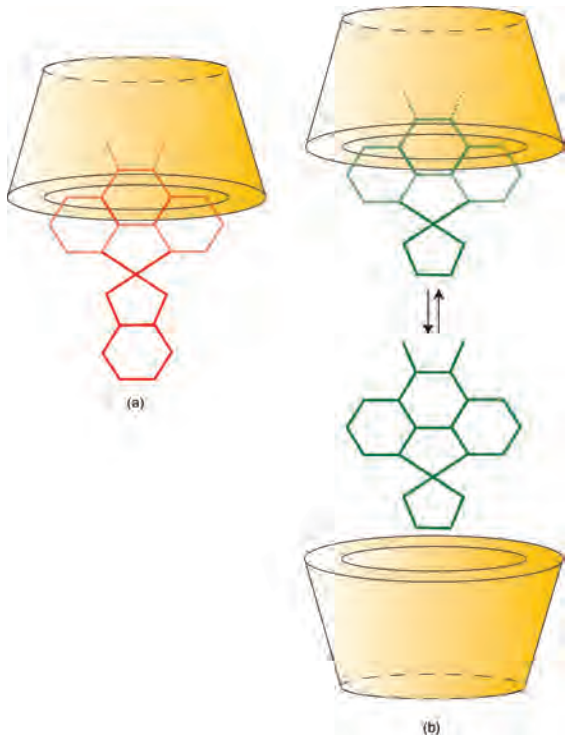

Figure 8. Diagrammatic representation of the 1:1 host−guest complexes formed with c-β-CD; (a) c-β-CD is bound over the phenanthroline ligand of **56MESS/56MERR**, and (b) also bound at the portal with the ethylenediamine ligand of **56MEEN**.

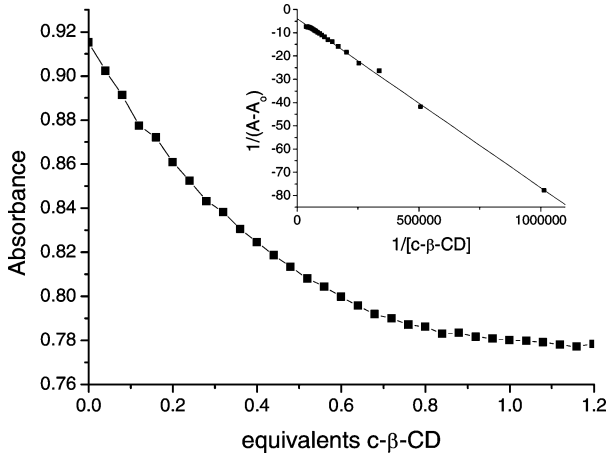

Figure 9. Plot of the absorbance of **56MESS** (at 229 nm) upon the addition of c-β-CD. The inset shows the double-reciprocal plot, indicating that a 1:1 encapsulation complex is formed.

Table 2. Binding Constants of the Metal Complexes **56MESS**, **56MERR**, and **56MEEN** to c-β-CD Determined from UV Titration Experiments and Analysed Using Four Different Mathematical Methods

	binding constant ($\times 10^4$ M^{-1})			
metal complex	Scatchard plot (eq *1*)	double-reciprocal plot (eq *2*)	nonlinear least-squares regression (eq *3*)	intrinsic method (eq *4*)
56MESS	5.9	5.4	7.9	23
56MERR	4.1	4.2	7.6	28
56MEEN	5.2	5.5	6.5	29

the ability of c-β-CD to stop degradation by glutathione was unexpected. We hypothesize that the steric bulk of the c-β-CD molecule over the phenanthroline is still able to prevent the approach of the *L*-glutathione molecule to the platinum center, thereby preventing degradation.

Table 3. Cytotoxicity of **56MESS** from 5 Day In Vitro Growth Inhibition Assays in the Absence and Presence of Equimolar Concentrations of s-CX[4] and c-β-CD in the LoVo Human Colorectal Cancer Cell Line

	IC_{50} (μM)[a]	
metal complex	1 h exposure	continuous exposure
56MESS	1.67 ± 0.39	0.13 ± 0.03
56MESS-s-CX[4]	2.18 ± 0.43	0.13 ± 0.06
56MESS-c-β-CD	1.83 ± 0.70	0.16 ± 0.03

[a] IC_{50} is defined as the concentration of metal complex required to inhibit cell growth by 50%.

Cytotoxicity. Because cucurbit[*n*]urils have previously been shown in some instances to significantly decrease the cytotoxicity of platinum(II)-based DNA intercalators, it was important to determine the effect of s-CX[4] and c-β-CD on the activity of **56MESS**. In vitro growth inhibition assays of **56MESS**, **56MESS** with s-CX[4], and **56MESS** with c-β-CD (1 equiv) were conducted against the LoVo (human colorectal cancer) cell line. With 1 h exposure of the cells to the metal complex, followed by 5 days incubation, s-CX[4] and c-β-CD were found to not affect the IC_{50} of **56MESS**, within the error of the experiment. In the continuous exposure experiment, again neither s-CX[4] or c-β-CD significantly affects the cytotoxicity of **56MESS** (Table 3). Overall, the results of the cytotoxicity experiments indicate that both c-β-CD and s-CX[4] may be suitable drug delivery vehicles for platinum(II)-based DNA intercalator complexes. Further research into the macrocycles including in vitro activity in cisplatin-resistant cell lines, particularly those with resistance derived from increased intracellular glutathione, is warranted.

Utility of the Macrocycles As Drug Delivery Vehicles. Previously, we have shown that CB[*n*]-metal complex complexes are poorly soluble in aqueous solvents; CB[8] is very insoluble and CB[6] requires large amounts of salt to attain sub-mM concentrations.[7] Only CB[7] host−guest complexes display acceptable solubility in water.[7] While s-CX[4] formed precipitates with the three metal complexes examined, the host−guest complexes of s-CX[4] are more soluble (**56MESS/56MERR** $\sim$ 0.1−0.2 mM, **56MEEN** $<$ 0.05 mM) than those for CB[*n*], and c-β-CD complexes are significantly more soluble than those of s-CX[4] (**56MESS/56MERR/56MEEN** $\sim$ 75 mM).

In addition to the better solubility of c-β-CD compared with s-CX[4], the chemistry of cyclodextrins, including their pharmacokinetics and pharmacodynamics, has been well studied, and there are already several pharmaceutical preparations that contain cyclodextrins.[20] The carboxylic acid groups of c-β-CD also allow the attachment of directing groups capable of recognizing and binding to the surface of cancer cells, using standard peptide coupling techniques. Such conjugated cyclodextrin drug delivery vehicles, while protecting the encapsulated drug from degradation, would also be able to target more specifically cancerous cells, and

(20) (a) Stella, V. J.; Rajewski, R. A. *Pharm. Res.* **1997**, *14*, 556–567. (b) Challa, R.; Ahuja, A.; Khar, R. K. *AAPS PharmSciTech* **2005**, *6*, E329E357. (c) Uekama, K.; Hirayama, F.; Arima, H. *J. Incl. Phenom. Macrocycl. Chem.* **2006**, *56*, 3–8.

thereby increase the drug's uptake and efficacy while reducing its adverse side-effects.

Conclusions

p-Sulfonatocalix[4]arene has been shown to encapsulate **56MESS**, **56MERR**, and **56MEEN**. **56MESS** and **56MERR** form 2:2 encapsulation complexes with s-CX[4], with two metal complex molecules associating in a head-to-tail type dimer, and with one s-CX[4] molecule encapsulated over either end. **56MEEN** also appears to form this complex initially, before undergoing a rearrangement reaction over time. Carboxylated-β-cyclodextrin has been shown to form 1:1 encapsulation complexes with **56MESS**, **56MERR**, and **56MEEN**, with the c-β-CD bound predominantly over the phenanthroline portion of the molecule. Encapsulation of **56MESS** by both s-CX[4] and c-β-CD was shown to decrease significantly the rate of metal complex degradation by reduced *L*-glutathione ($t_{1/2} > 9$ days). No significant difference was observed in the cytotoxicity in the LoVo colorectal cancer cell line of **56MESS** when encapsulated within either s-CX[4] or c-β-CD. Because neither macrocycle significantly decreased the cytotoxicity of **56MESS**, both have potential as drug delivery vehicles. The increased solubility of the metal complexes with c-β-CD compared with s-CX[4] and the useful carboxylic acids groups of c-β-CD mean this macrocycle is the best candidate to take forward to study in further in vitro trials, particularly with a range of cancer cell lines with resistance to platinum drugs from increased intracellular glutathione concentrations.

Acknowledgment. A. M. Krause-Heuer was supported by a University of Western Sydney Vice Chancellor's Leadership Scholarship and a College of Health and Science Publication Fellowship. We thank Northern Cancer Institute, U.K. for kindly providing the facilities and materials to conduct the biological testing, and Janki J. Rami for conducting preliminary biological testing. We thank Professor William S. Price for his assistance in conducting PGSE experiments.

IC800467C